



*Anal. Bioanal. Chem. Res., Vol. 10, No. 1, 15-23, January 2023.*

## **Disposable Paper-based Biosensing Platform for Procalcitonin Detection**

Yachana Gupta and Aditya Sharma Ghrera\*

*Applied Science Department, The NorthCap University, Gurugram, India*

*(Received 7 May 2022, Accepted 16 August 2022)*

Procalcitonin (PCT) plays a significant role in screening for bacterial infection (BI), which is one of the world's leading health issues. This work presents a simple, efficient, and convenient glass fiber paper (GFP) substrate-based innovative biosensor application for BI-specific PCT biomarker detection. To enhance the conductivity of the GFP substrate, a self-accumulating single layer of AuNP is used on the GFP surface. This monolayer of AuNP in GFP provides a platform for antibody immobilization and shows high electrochemical conductivity. Further, the AuNP/GFP electrode was modified with antibodies specific to PCT, followed by the addition of bovine serum albumin (BSA) to block unspecific binding sites for PCT detection. The PCT/BSA/ab/AuNP/GFP bioelectrode has been successfully used to determine PCT in a serum sample with amended stability. The structural and morphological features were characterized using scanning electron microscopy, transmission electron spectroscopy, Fourier transforms infrared, ultraviolet-visible spectroscopy, and X-ray diffraction. Using an electrochemical impedance response study, the developed PCT/BSA/ab/AuNP/GFP bioelectrode showed the lowest detection limit of 100 pg ml<sup>-1</sup> concerning PCT detection in the linear range of 10<sup>7</sup>-10<sup>2</sup> pg ml<sup>-1</sup>. Electrochemical response studies show that the developed BSA/ab/AuNP/GFP bioelectrode has a lifespan of 30 days and can be used to assess PCT in the 10<sup>7</sup>-10<sup>2</sup> pg ml<sup>-1</sup> range. Moreover, this evaluated sensor offers many merits, including a lower cost, small sample volume, single-use, and rapid analysis over conventional methods, making this platform an alternative option for PCT screening. This designed bioelectrode also shows adequate reproducibility.

**Keywords:** Electrochemical impedance spectroscopy, Gold nanoparticles, Glass fiber paper monoclonal antibody, Procalcitonin

### **INTRODUCTION**

According to the World Health Organization (WHO), disease-causing bacteria are one of the greatest threats to public health and will continue to be the most dangerous as antibiotic resistance rises. Over the earlier span, many research methods have been developed to detect bacterial infection (BI), and several studies have shown a parallel relationship between high serum PCT levels and patients with positive BI and sepsis. During BI or sepsis, PCT acts as a precursor for the hormone calcitonin and can distinguish between viral and bacterial infections and other infections caused by the inflammatory condition [1]. The molecular weight of the PCT hormone is 14.5 kDa, containing 116

amino acid peptides. It is used in several clinical settings. During BI, the PCT level increases and falls rapidly from normal concentration so that diagnosis is possible to monitor the infections in a timely. In healthy individuals, serum PCT concentrations are less than 0.05 µg l<sup>-1</sup> [2]. For concentrations 0.05-0.5 µg l<sup>-1</sup> local infection is possible, and as the concentration increases, the likelihood of systematic infection also increases. For concentrations greater than 10 µg l<sup>-1</sup> servers, bacterial sepsis or septic shock is highly possible. The spread of these infectious diseases requires the development of biosensors for their detection, timely observation, and monitoring. Biosensors provide high specificity, minimal use of chemicals needed for calibration, fast response times, and the ability to quantify nonionic substances that cannot be evaluated with other traditional devices [3,4]. In recent years, electrochemical biosensors

\*Corresponding author. E-mail: adityasghrera@gmail.com

have shown a significant role in the detection of BI [5]. Electrochemical detection is an attractive technique due to its quantifiable ability. Currently, glassy carbon, gold-plated glass electrodes are used to develop the desired biosensing platform. However, these biosensing platforms showed various limitations, such as high cost, rigidity, and the need for pretreatments [6]. The latest paper-based biosensing platform has attracted more attention to point-of-care (POC) detection due to its high sensitivity, flexibility, small sample volume requirements, fast response, etc. Some of the previously reported work done by research groups on PCT detection led to the development of an effortless, portable, and economical advanced method based on a paper substrate, such as Zhan *et al.* reported cellulose membrane-based lateral flow assay (LFA) technology for PCT and C-reactive protein (CRP) detection with a limit of detection (LOD) of  $0.12 \text{ ng ml}^{-1}$  and  $0.24 \text{ } \mu\text{g ml}^{-1}$ , respectively [7]. Serebrennikova *et al.* reported LFA-based PCT detection using gold nanopopcorns with  $0.1 \text{ ng ml}^{-1}$  LOD [8]. In addition, electrochemical biosensors can provide information on the redox stability of paper-based sensors, anti-extraction stability, and resistance to biofouling, and it is also possible to monitor the effectiveness of modification through the usage of nanocomposites [9] such as gold nanoparticles (AuNP) [10], carbon nanotubes, and magnetic particles [11]. AuNP is used in various paper-based sensor developments because of its biocompatibility, large surface area, low cytotoxicity, and stability. Electrochemical techniques, particularly electrochemical impedance spectroscopy (EIS), have drawn much attention in developing paper-based sensors as POC biosensors. By a low impedance response at specific frequencies and measuring the resulting small electrical current, EIS measures the impedance between two conductive materials of an electrochemical cell. EIS is a label-free, actual, experimental technique because the impedance changes as a consequence of proteins (analytes) interacting with ligands deposited on the electrode surface. Such properties are significant in POC applications where it is necessary to reduce detection time, reagents, and assay steps. EIS retains too much potential for versatile immunodiagnostic platforms because it does not require secondary labeling or washing, in contrast to other surface-based affinity assays, such as the conventional enzyme-

linked immunosorbent assay (ELISA), which require rinsing steps to eliminate non-covalently analytes, ligands, and labels [12-14]. Numerous reports have been published on EIS for the detection of a variety of biomarkers. Lim *et al.* evaluated an electrochemical biosensor for the detection of PCT. To monitor the performance of the sensor, cyclic voltammetry (CV) and EIS studies were used [15]. In the developed biosensor, an Au electrode was used, which increased the cost and also required experience to handle. Boonkaew *et al.* developed a paper-based electrochemical biosensor for PCT and other biomarker detection [16]. This proposed sensor can be used for POC detection but with this sensor, proteins cannot be directly detected often there is a need for quantification of chemical labeling. Zupanacic *et al.* evaluated nanocomposite coated electrochemical detection for multiplexed detection of sepsis biomarkers (PCT, CRP) in the  $\text{ng ml}^{-1}$  and  $\mu\text{g ml}^{-1}$  ranges [17]. Dendrimer-encapsulated AuNP, based on an enzyme-free electrochemical immunosensor was evaluated by Wen-Jun Shen *et al.* for PCT determination in the linear range from  $500 \text{ ng ml}^{-1}$  to  $1.80 \text{ pg ml}^{-1}$  [18]. In the literature mentioned above, electrochemical biosensors for PCT detection have been developed. However, they are expensive, inconvenient for storage, and on the surface of other electrodes, the antigen-antibody interaction is too weak and cannot be retained on the surface for further use. Thus, there is a need to make a cost-effective, disposable, and simple biosensor platform with good interaction of antigen-antibody on the surface of electrodes towards PCT detection.

The present report evaluates a novel, flexible, portable, and accessible electrochemical biosensor for PCT detection. For the modification of the paper-based biosensing platform, glass fiber paper (GFP) was used as a substrate. To evaluate the good combination of nanointerface and electrode material, as well as the performance of the sensor platform on flexible and disposable glass fiber substrates, is being actively pursued to develop a POC device for PCT detection. It fulfils the requirements of modern POC diagnosis and detects BI quantitatively. It is helpful to provide a microfluidic testing platform due to their hydrophobic interaction. This biosensor exhibited amended stability (92.4%), reproducibility (2.6%), and a  $100 \text{ pg ml}^{-1}$  detection limit.

## EXPERIMENTAL

### Chemicals and Reagents

Sodium citrate tribasic dihydrate, chloroauric acid, bovine albumin serum (BSA), monobasic sodium phosphate, and Disodium phosphate were purchased from CDH Chemicals. Tween-80 and sodium borohydride were purchased from Thomas Baker (Chemicals), while Mab was purchased from mybiosource.com. Glass fiber paper (24 × 260 mm) was procured with an advanced micro device (MDI) membrane.

### Fabrication of Glass Fiber Paper Strips (GFP)

The glass fiber paper was cut into (2.3 × 1.4 cm<sup>2</sup>) dimension strips. These strips were pretreated with 3-4 drops of Tween 80 detergent solution in 25 ml of deionized water, followed by washing with an excess amount of water and ethanol. The strips were then desiccated in the oven at 37 °C for 15 min. AuNP was synthesized by the citrate stabilized method previously reported in our research paper [19]. For AuNP deposition, the dried strips were immersed in 5 ml of 2.5 mM citrate stabilized [20-22] AuNP solution for 24 h, followed by air-drying for 30 min [23]. Hydroxyl group (OH), a chemical moiety present on the AuNP, may facilitate its adsorption on the borosilicate fibers through hydrogen

bonding [24-27]. As prepared, AuNP by the citrate stabilized method broad peak was observed at 3296 cm<sup>-1</sup> which was related to water intermolecular interaction with a free carboxylic acidic group of the absorbed citrate anions on AuNP. It was confirmed with the FTIR spectrum [28,29].

AuNP-treated GFP turned from colorless to a red color. In Fig. S1, the deposition of AuNP (ruby red color) was observed after dipping GFP in AuNP solution. AuNP is commonly stabilized through the absorption of a dispersant layer of buffers around the particle surface. Buffers regulate pH shifts upon the addition of acidic or basic components. They can also stabilize proteins. It can neutralize small amounts of added acid or base, thus keeping the solution's pH relatively stable. Buffers were used as pretreatment of GFP to control the sample's flow rate and make it suitable for interaction with the AuNP. After AuNP deposition, 10 μl of Mab (anti-PCT) was dropped and dried for 15 min. AuNP will bind some of the antibody sites, while BSA will block the leftover sites of anti-PCT over GFP because it was used as a blocking agent for non-specific binding. Then, 10 μl of pre-prepared concentrations of antigen PCT were dropped onto the surface individually. EIS studies were conducted using the prepared bioelectrode. Figure 1 depicts the development of a paper sensor.

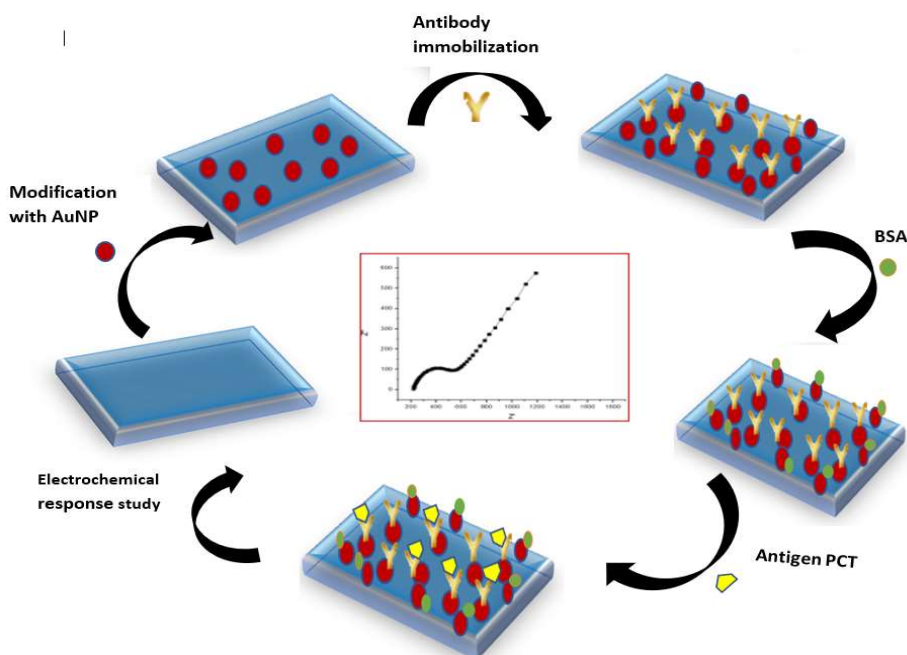
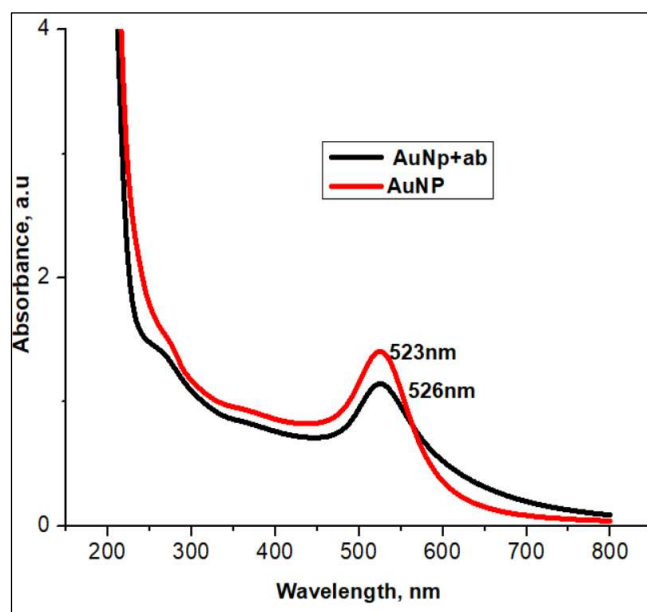


Fig. 1. Development of GFP sensor for PCT detection.

## RESULTS AND DISCUSSION

### Characterization

To characterize AuNP and their conjugates, studies in the ultraviolet and visible (UV-Vis) spectral regions, transmission electron microscopy (TEM), and scanning electron microscopy (SEM) have been carried out. The UV-Vis spectroscopy presented a  $\lambda_{\max}$  value of 523 nm, which presented a bathochromic shift at 526 nm after conjugation with monoclonal antibody (mAb) (Fig. 2a). The synthesized particles were further characterized by the TEM technique (Fig. 3a). The prepared AuNP solution was dropped (10  $\mu$ l) onto a copper grid that was coated with carbon. The grid was allowed to dry in atmospheric conditions. TEM characterization presented the size range of AuNP at 10 nm. However, most of the particles were in the size range of 20-23 nm, confirming the monodispersity of the synthesized particles. SEM (JEOL JSM-7610F plus) was used for the morphological characterization of AuNP.



**Fig. 2.** UV-Vis absorption spectrum of AuNP and conjugate (AuNP-mAb).

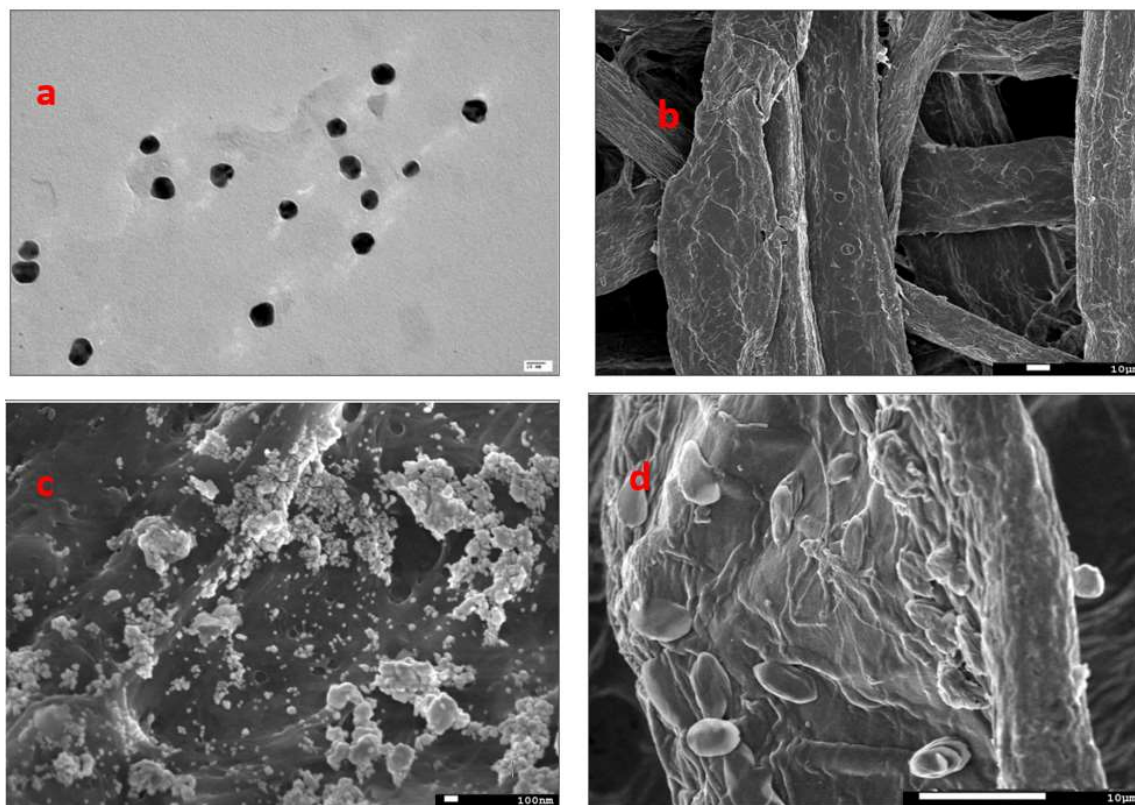


**Fig 3.** (a) TEM image of AuNP, (b) SEM image of GFP substrate, (c) SEM image of AuNP/GFP, (d) SEM image of ab/AuNP/GFP.

To study the dispersion and particle separation on a solid substrate, SEM characterization was studied. For this analysis, the GFP substrate was washed with Tween 80 surfactant, stirred for 10 minutes, and dried. The cleaned GFP substrate SEM image is shown in Fig. 3b. There after, synthesized AuNP was coated 4 times. Each coating was done with 10  $\mu\text{l}$  of AuNP onto the surface of the GFP substrate. After that, the substrate was dried and used for SEM analysis. With the help of SEM, spherical-shaped particles were observed (Fig. 3c), and after the successfully deposited AuNP, 10  $\mu\text{l}$  of anti-PCT (Mab) was dropped and dried (Fig. 3d).

### FT-IR and XRD Analysis

The FT-IR measurements provided evidence of the surface covalent functionalization of AuNP by the citrate method (Fig. 4a). AuNP's FTIR analysis reveals broad and strong characteristic absorption at 3296, 2129, and 1637  $\text{cm}^{-1}$  [30], which correspond to the asymmetric stretching of  $-\text{OH}$ ,  $-\text{C}=\text{O}$  (carbonyl), and C-O (epoxy) groups, respectively [31]. These findings support the interplay of citrate ions with AuNP. The emergence of three-dimensional AuNP strongly depends on stabilizing citrate ions at the surface. Surface functionalization of AuNP with citrate ions can be carried out systematically.

The X-ray diffraction (XRD) technique was used to investigate the crystallinity of synthesized AuNPs, and the

corresponding spectra are shown in Fig 4b. Gold nanoparticles decided to show four distinct peaks at  $2\theta = 22.5^\circ$ ,  $38.4^\circ$ ,  $44.4^\circ$ , and  $71.3^\circ$ . All four peaks correspond to orthorhombic lattice conventional Bragg reflections (040), (061), (200), and (111). The shape of the crystal is determined by the seven crystal parameters ( $a \neq b \neq c$ ,  $\alpha = \beta = \gamma = 90^\circ$ ). The intense refraction at the 38.4 peaks indicates that zero-valent gold's preferred growth perspective was fixed in the (061) direction [32,33]. This term refers to molecular-sized solids made up of a reiterating 3D sequence of atoms or molecules with equal distances between each part. This XRD pattern is a distinguishing feature of pure Au nanocrystals. The Scherrer formula is often used to compute the average size of a crystal in the vertical plane  $D = K\lambda/(\beta\cos\theta)$ , where  $K = 0.94$  is the X-ray wavelength for cubic crystal structure and  $d$  is the full thickness at half the peak's maximum intensity (Radians).

### Electrochemical Characterization

An Autolab PGSTAT204 galvanostat/potentiostat (EcoChemie, Netherlands) was used to carry out all electrochemical characterization. All electrochemical experiments were carried out with a three-electrode system using paper modified with AuNP (AuNP/GFP) as a working electrode, platinum foil as a counter electrode in 0.1 M KCl containing 10 mM  $[\text{Fe}(\text{CN})_6]^{-3/4}$  redox probe and Ag/AgCl were used as reference electrodes.

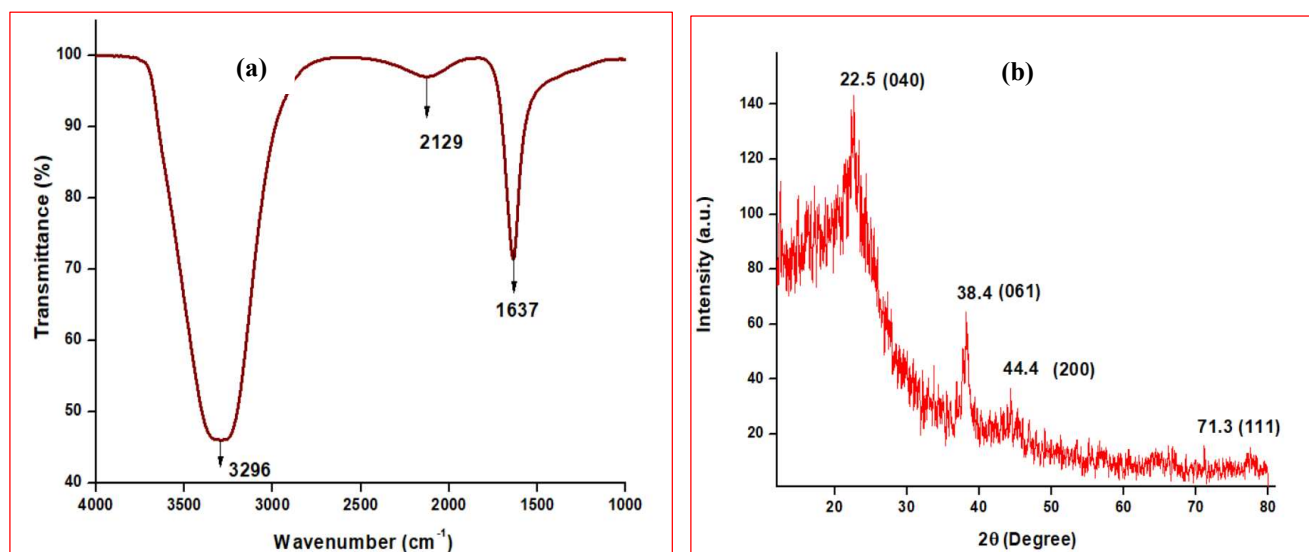
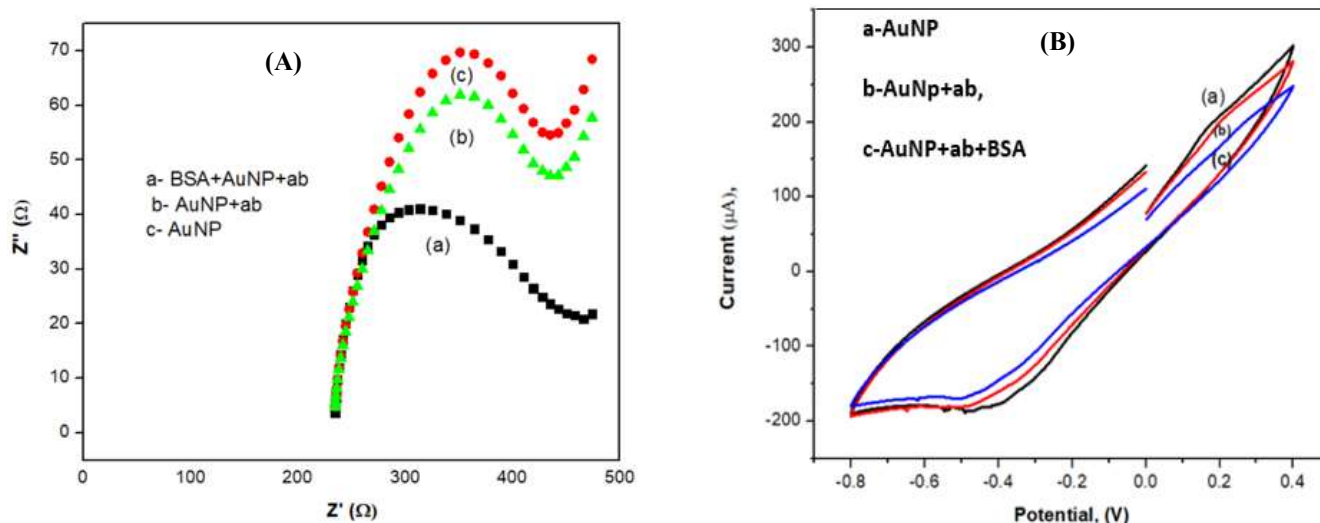


Fig. 4. (a) and (b) FTIR and XRD spectra of AuNP.

EIS is one of the most widely used emission experimental techniques that help to elucidate the behavior of electrochemical systems and therefore allows the analysis of multiple phenomena within a cell. The meaning of the EIS is the measurement of resistance given by a circuit to a current when electricity is applied. The EIS method elicits a reaction based on a phase change or a change in temperature in the fluid or applied current, which brings the electrode to a state far from equilibrium. Electrical resistance is measured in an electrochemical cell by applying an alternating potential. EIS is a variety of electrochemical methods, which can be used as faradaic or non-faradaic processes and can study the physical properties, test processes [34,35], or biorecognition events at the electrode surface. Herein, the GFP surface is modified with AuNP. Each modified electrode was estimated on the scale of a semicircle. In Fig. 5a, after the modification with AuNP onto the GFP surface, the value of  $R_{ct}$  293.87 $\Omega$  (Curve c) was observed. The increased value of  $R_{ct}$  reveals the fast electron transference compared to the GFP electrode (Fig. S2). The  $R_{ct}$  value further increases and reaches 312.64  $\Omega$  (curve b). This proves that monoclonal antibodies (Mab) are effectively immobilized on the surface. The other reason may be an increase in the kinetic barrier for electron transfer. The  $R_{ct}$  value increases significantly with the addition of the BSA blocking agent 327.99  $\Omega$  (curve a). Here, BSA acts as an obstructive agent for unspecific binding sites and acts as

an insulator. Therefore, BSA interferes with electron transfer, resulting in the  $R_{ct}$  value increasing on the curved [36-39]. These relative changes in  $R_{ct}$  values of different electrodes maintain the modification of the corresponding electrodes. The obtained results of EIS showed that the GFP-based sensing platform was successfully developed and working properly in detecting procalcitonin.

The electrochemical behavior of a modified bioelectrode (BSA/ab/AuNP/GFP) with various PCT concentrations was also recorded by cyclic voltammetry (CV) in a 10 mM  $[\text{Fe}(\text{CN})_6]^{3-/4-}$  redox probe containing 0.1 M KCl solution in the potential range from -0.8 to 0.4 V at a scan rate of 50  $\text{mV s}^{-1}$ . For the study of the surface of the modified paper electrode, CV is an effective and valuable method [40, 41]. So, CV was selected to examine the change in behavior of paper electrodes after modification with the AuNP. Figure 5b reveals the CV of the (a) AuNP/GFP, (b) ab/AuNP/GFP, and (c) BSA/ab/AuNP/GFP bioelectrode at a scan rate of 50  $\text{mV s}^{-1}$  in a potential range of -0.8 to 0.4 V. Both anodic and cathodic peak currents are measured after and before modifications. Figure 5b [curve (b)] shows the electrochemical behavior of a paper electrode. After modification of the GFP substrate with AuNP, it shows a peak current value of 210.69  $\mu\text{A}$  due to electron transfer from AuNP on the GFP surface, and the bare GFP surface has been presented in Fig. S3. In curve (b), a peak current of



**Fig. 5.** Electrochemical (A) EIS (a) BSA/ab/AuNP/GFP, (b) ab/AuNP/GFP (c) AuNP/GFP, and (B) CV studies conducted on the modified paper electrode (a) AuNP/GFP, (b) ab/AuNP/GFP, and (c) BSA/ab/AuNP/GFP.

198.38  $\mu\text{A}$  is observed, which is lower than that of the AuNP-modified electrode due to the immobilization of antibodies on the paper surface [42]. When blocking agent BSA is used for further modification, the current value decreases and reaches 169.22  $\mu\text{A}$ . This is because BSA, being shielded in nature, prevents electron transference between the medium and the electrode, decreasing the peak current value [42]. Relative changes in current strength influenced the presence of PCT on the surface of the paper.

### Impedance Sensing Study of GFP Strips: Conducting Strips

The electrochemical response studies of the PCT/BSA/ab/AuNP/GFP bioelectrode [presented in Fig.6 (a)] were conducted as a function of antigen PCT concentration  $10^7$  to  $10^2$   $\text{pg ml}^{-1}$  in 10 mM  $[\text{Fe}(\text{CN})_6]^{3-/4-}$  and 0.1 M KCl redox probe using EIS study. For this purpose, BSA was used as an obstructive agent for unspecific interaction for sensing responses. The current value was examined with the addition of each PCT concentration, the current value was examined. Electrically insulated antibody-antigen complexes are formed due to the specific interaction between PCT and anti-PCT, which shows a decrease in current value, and may reduce the charge transfer of  $[\text{Fe}(\text{CN})_6]^{3-/4-}$ . The reduction in the amperometric current at the surface of the electrode was predicted [35]. In Fig. 6a, the

$R_{ct}$  of GFP sensing electrodes of PCT concentration is calculated by the diameter of a semicircle, signified by a slow electron transfer of PCT on GFP sensing electrodes [35]. Regular decreases in the kinetic barrier for electron transfer were noticed in the range of  $10^7$  to  $10^2$   $\text{pg ml}^{-1}$  of PCT concentration which shows the decrease in  $R_{ct}$  values. Figure 6b shows the calibration curve obtained in the range of  $10^7$  to  $10^2$   $\text{pg ml}^{-1}$  of the PCT concentration. The response current and impedance biosensor calibration line covered the required detection range. It was found that the logarithmic value of PCT concentrations and  $R_{ct}$  variation have a linear correlation within a range of  $10^7$  to  $10^2$   $\text{pg ml}^{-1}$ , which is appropriate for PCT concentrations. The LOD of the developed sensor was found to be  $100 \text{ pg ml}^{-1}$ , with a linear correlation coefficient of 0.979.

### Stability and Reproducibility

Stability and reproducibility were evaluated by the EIS technique. To monitor the biosensor's stability, the response current of the fabricated bioelectrode BSA/ab/AuNP/GFP was measured every five days. After 30 days, the fabricated BSA/ab/AuNP/GFP bioelectrode retained approximately 92.4% of the initial current response, demonstrating that the BSA/ab/AuNP/GFP bioelectrode is stable (Fig. 7a). The percentage of  $R_{ct}$  observed (7.6%) for the six consecutive measurements was within a reasonable and acceptable range.

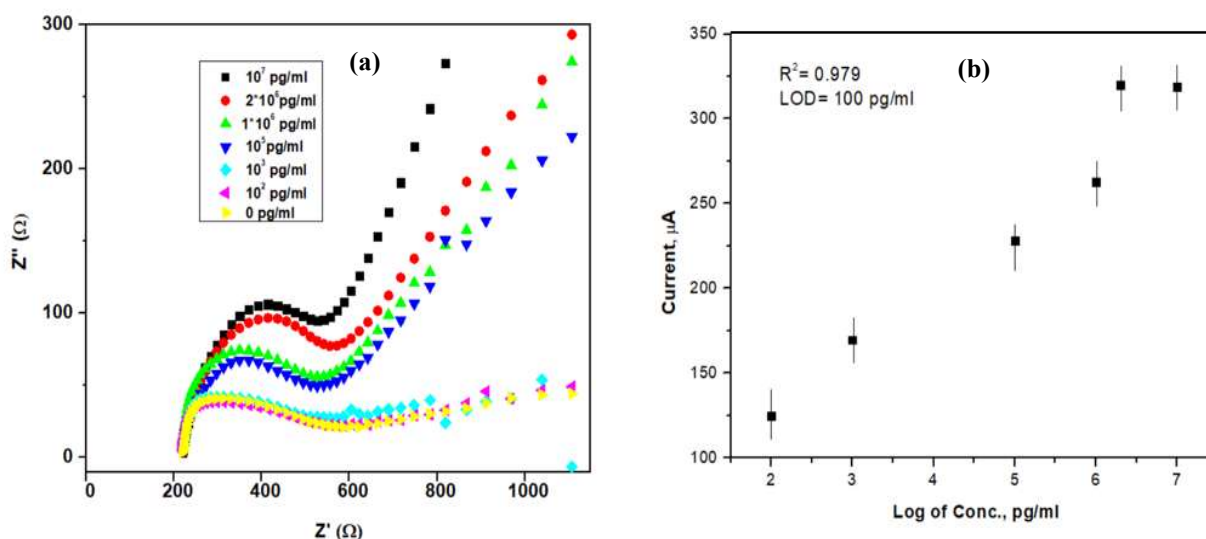


**Fig. 6.** (a) Electrochemical response study of PCT/BSA/ab/AuNP/GFP bioelectrode in 0.1 M KCl containing 10 mM  $[\text{Fe}(\text{CN})_6]^{3-/4-}$  redox probe using EIS. (b) Linear calibration of the PCT/BSA/ab/AuNP/GFP bioelectrode between the value of PCT concentrations and peak current.

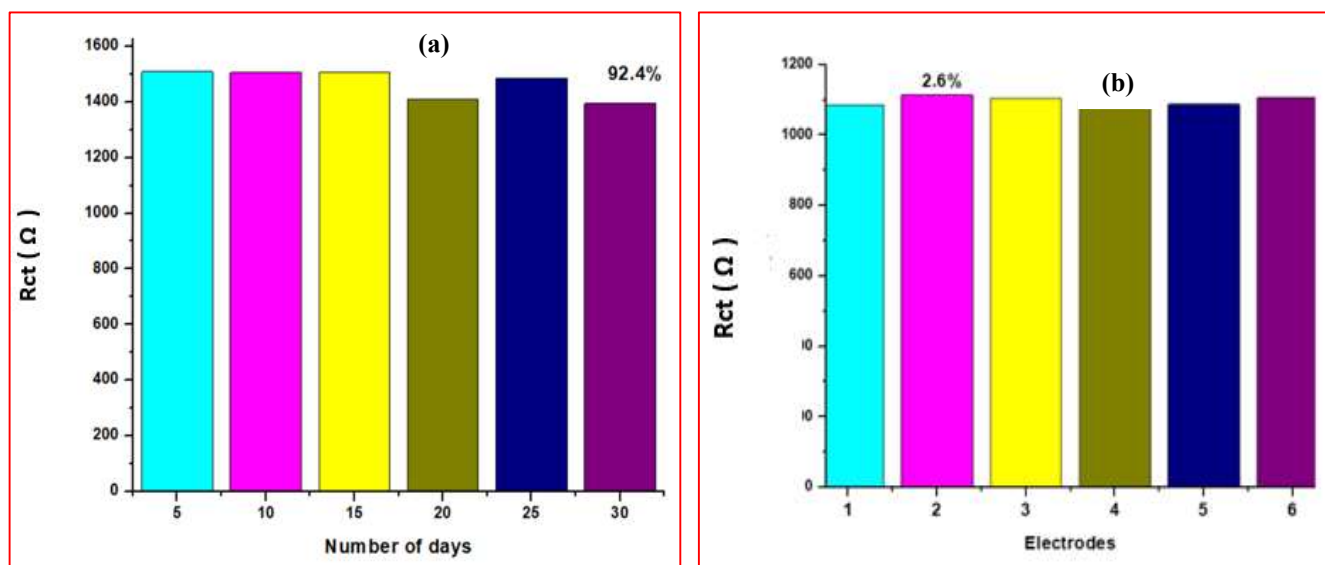


**Fig. 7.** a and b Stability and reproducibility curve of the BSA/ab/AuNP/GFP bioelectrode in KCl containing  $[\text{Fe}(\text{CN})_6]^{3-/4-}$ .

This enhanced stability is due to the strong affinity between AuNP and GFP, which is introduced due to repeated pretreatment. To assess reproducibility, six different BSA/ab/AuNP/GFP bioelectrodes were modified under similar conditions. A small change in current was predicted, proving that the BSA/ab/AuNP/GFP bioelectrode (Fig. 7b) showed good reproducibility with a relative standard deviation of 2.6% for six different bioelectrodes.

## CONCLUSIONS

In this work, a simple, cost-effective, ecological, and disposable GFP-based biosensing platform was fabricated for the electrochemical detection of PCT. The GFP-based paper electrode showed a suitable electrode surface for covalent immobilization of antigen-antibody. Herein, AuNP is used as a modifying agent of GFP due to its good biocompatibility with the paper surface. The fabricated PCT/BSA/ab/AuNP/GFP bioelectrode revealed a low detection limit of  $100 \text{ pg ml}^{-1}$ . To the best of our knowledge, no other group has reported an AuNP/GFP-based biosensor for the detection of PCT. This extremely flexible, portable, user-friendly GFP electrode has been employed, which shows good stability and reproducibility towards PCT detection.

## ACKNOWLEDGMENTS

The authors acknowledge the support from The authors wish to thank and acknowledge AIRF- JNU for the TEM characterization and acknowledge the support from Manipal University, Jaipur for the FESEM, EDAX, XRD, and FTIR characterization and acknowledge The NorthCap University for UV-Vis characterization.

## REFERENCES

- [1] S. Sahu, G. Dutta, *Sensors International* 2 (2021) 100107.
- [2] R.H. Snider, E.S. Nylén, K.L. Becker, *J. Investig. Med.* 45 (1997) 552.
- [3] Y. Gupta, A.S. Ghrera, *Archiv. Micro. Biol.* 203 (2021) 3767.
- [4] X.-Y. Shao, C.-R. Wang, C.-M. Xie, X.-G. Wang, R.-L. Liang, W.-W. Xu, *Sensors (Basel)* 17 (2017) 480.
- [5] F. Otero, E. Magner, *Sensors (Basel)* 20 (2020) 3561.
- [6] S. Carrara, S. Ghoreishizadeh, J. Olivo, I. Taurino, C. Baj-Rossi, A. Cavallini, M.O. de Beek, C. Dehollain, W. Bursleson, F.G. Moussy, A. Guiseppi-Elie, G. De Micheli, *Sensors (Basel)* 12 (2012) 11013.
- [7] N. Zhan, Y. Zhou, L. Mei, Y. Han, H. Zhang, *Anal. Sci.* 35 (2019) 257.

- [8] K. Serebrennikova, J. Samsonova, A. Osipov, *Nanomicro Lett.* 10 (2017) 24.
- [9] S. Nellaiappan, P. K. Mandali, A. Prabakaran, U.M. Krishnan, *Chemosensors* 9 (2021) 182.
- [10] F. Yuan, T. Liao, H. Yu, Z. Li, *Anal. Methods* 8 (2016) 1577-1585.
- [11] Á. Molinero-Fernández, M. Moreno-Guzmán, M.Á. López, A. Escarpa, *Biosensors* 10 (2020) 66.
- [12] Xiaowen Liu, Lin Li Andrew, J. Mason, *Philos. Trans. Royal Soc.* 372 (2012) 372.
- [13] J.S. Daniels, N. Pourmand, *Electroanalysis* 19 (2007).
- [14] H.S. Magar, R.Y.A. Hassan, A. Mulchandani, *Sensors (Basel)* 21 (2021) 6578.
- [15] J.M. Lim, M.Y. Ryu, J.H. Kim, C.H. Cho, T.J. Park, J.P. Park, *RSC Advan.* 7 (2017) 36562.
- [16] S. Boonkaew, I. Jang, E. Noviana, W. Siangproh, O. Chailapakul, C.S. Henry, *Sens. Actuators B Chem.* 330 (2021) 129336.
- [17] U. Zupančič, P. Jolly, P. Estrela, D. Moschou, D.E. Ingber, *medRxiv.* (2020) 2011.3.20224683.
- [18] W.-J. Shen, Y. Zhuo, Y.-Q. Chai, Z.-H. Yang, J. Han, R. Yuan, *ACS Appl. Mater. Interfaces.* 7 (2015) 4127.
- [19] Y. Gupta, Kalpana, A.S. Ghreera, *J. Electrochem. Sci. Eng.* 12 (2022) 265.
- [20] J. Turkevich, P.C. Stevenson, J. Hillier, *Discuss. Faraday Soc.* 11 (1951) 55.
- [21] J. Dong, P.L. Carpinone, G. Pyrgiotakis, P. Demokritou, B.M. Moudgil, *Kona.* 37 (2020) 224.
- [22] P. Suchomel, L. Kvitek, R. Pucek, A. Panacek, A. Halder, S. Vajda, R. Zboril, *Sci. Rep.* 8 (2018) 4589.
- [23] Y.H. Nago, Li. Dan, P. George, S.G. Garnier., *Langmuir* 28 (2012) 8782.
- [24] A. Gupta, V. Mishra, R. Srivastava, *Nano Express*, 1(2020) 010048.
- [25] D.Deng, Q. Lin, H. Li, Z. Huang, Y. Kuang, H. Chen, J. Kong, *Talanta* 200 (2019) 272.
- [26] K. Shrivastava, Bhuneshwari Sahu, M. Deb, S.S. Thakur, Sushama Sahu, Ramsingh Kurrey, T. Kant, T. Patle, R. Jangde, *Microchem. J.* 150 (2019) 104156.
- [27] T. Ye, Z. Huang, Z. Zhu, D. Deng, R. Zhang, H. Chen, *Talanta* 220 (2020) 121357.
- [28] A. Boldeiu, M. Simion, L. Mihalache, A. Radoi, M. Banu, P. Varasteanu, P. Nadejde, E. Vasile, A. Acasandrel, R. Cristina, D. Savu, M. Kusko., *J. Photochem. Photobiol. B, Biol.* 197 (2019) 111519.
- [29] Y.H. Ngo, D. Li, G.P. Simon, G. Garnier, *Langmuir* 28 (2012) 8782.
- [30] J.V. Piovesan, E.R. Santana, A. Spinelli, *J. Electroanal. Chem.* 813 (2018) 163.
- [31] B. Amanulla, S. Palanisamy, S.-M. Chen, T.-W. Chiu, V. Velusamy, J.M. Hall, T.-W. Chen, S.K. Ramaraj, *Sci. Rep.* 7 (2017) 14182.
- [32] K. Sneha, M. Sathishkumar, S. Kim, Y.-S. Yun, *Process Biochem.* 45 (2010) 1450.
- [33] S. Krishnamurthy, A. Esterle, N.C. Sharma, S. V. Sahi, *Nano. Res. Lett.* 9 (2014) 627.
- [34] A.S. Tanak, B. Jagannath, Y. Tamrakar, S. Muthukumar, S. Prasad, *Anal. Chim. Acta* 3 (2019) 100029.
- [35] X. Li, Z. Qin, H. Fu, T. Li, R. Peng, Z. Li, J.M. Rini X. Liu, *Biosens. Bioelectron.* 177 (2021) 112672.
- [36] J. Narang, N. Malhotra, C. Singhal, A. Mathur, D. Chakraborty, A. Anil, A. Ingle, C.S. Pundir, *Biosen. Bioelectron.* 88 (2017) 249.
- [37] N. Ruecha, K. Shin, O. Chailapakul, N. Rodthongkum, *Sens. Actuators B Chem.* 279 (2019) 298.
- [38] S. Kumar, A. Sen, S. Kumar, S. Augustine, B.K. Yadav, S. Mishra, B.D. Malhotra, *App. Phys. Lett.* 108 (2016) 203702.
- [39] H. Li, S. Song, M. Wen, T. Bao, Z. Wu, H. Xiong, X. Zhang, W. Wen, S. Wang, *Biosen. Bioelectron.* 142 (2019) 111532.
- [40] G. Zhao, G. Liu, *J. Nanomater.* 9 (2019) 31-47.
- [41] J.A. Buledi, S. Ameen, N.H. Khand, A.R. Solangi, I. H. Taqvi, M.H. Agheem, Z. Wajdan, *Electroanalysis* 32 (2020) 1600.
- [42] P. Lv, L. Min, R. Yuan, Y. Chai, S. Chen, *Microchim. Acta* 171 (2010) 297.